A highly contiguous genome assembly of red perilla (*Perilla frutescens*) domesticated in Japan

Keita Tamura[1,2], Mika Sakamoto[3], Yasuhiro Tanizawa[3], Takako Mochizuki[3], Shuji Matsushita[4], Yoshihiro Kato[5], Takeshi Ishikawa[5], Keisuke Okuhara[1,6], Yasukazu Nakamura[3], Hidemasa Bono[1,2*]

[1]Laboratory of Genome Informatics, Graduate School of Integrated Sciences for Life, Hiroshima University, 3-10-23 Kagamiyama, Higashi-Hiroshima, Hiroshima 739-0046, Japan

[2]Laboratory of BioDX, Genome Editing Innovation Center, Hiroshima University, 3-10-23 Kagamiyama, Higashi-Hiroshima, Hiroshima 739-0046, Japan

[3]Genome Informatics Laboratory, Department of Informatics, National Institute of Genetics, 1111 Yata, Mishima, Shizuoka 411-8540, Japan

[4]Agricultural Technology Research Center, Hiroshima Prefectural Technology Research Institute, 6869 Hara, Hachihonmatsucho, Higashi-Hiroshima, Hiroshima 739-0151, Japan

[5]Mishima Foods Co., Ltd., 3-10-7 Kanonshinmachi, Nishi-ku, Hiroshima City, Hiroshima 733-0036, Japan

[6]PtBio Inc., 3-10-23 Kagamiyama, Higashi-Hiroshima, Hiroshima 739-0046, Japan

Running Head: Genome sequencing of *Perilla frutescens*

*Correspondence: bonohu@hiroshima-u.ac.jp; Tel.: +81-82-424-4013

Abstract

Perilla frutescens (Lamiaceae) is an important herbal plant with hundreds of bioactive chemicals, among which perillaldehyde and rosmarinic acid are the two major bioactive compounds in the plant. The leaves of red perilla are used as traditional Kampo medicine or food ingredients. However, the medicinal and nutritional uses of this plant could be improved by enhancing the production of valuable metabolites through the manipulation of key enzymes or regulatory genes using genome editing technology. Here, we generated a high-quality genome assembly of red perilla domesticated in Japan. A near-complete chromosome level assembly of *P. frutescens* was generated contigs with N50 of 41.5 Mb from PacBio HiFi reads. 99.2% of the assembly was anchored into 20 pseudochromosomes, among which seven pseudochromosomes consisted of one contig, while the rest consisted of less than six contigs. Gene annotation and prediction of the sequences successfully predicted 86,258 gene models, including 76,825 protein-coding genes. Further analysis showed that potential targets of genome editing for the engineering of anthocyanin pathways in *P. frutescens* are located on the late-stage pathways. Overall, our genome assembly could serve as a valuable reference for selecting target genes for genome editing of *P. frutescens*.

Keywords

Perilla frutescens, genome assembly, PacBio HiFi reads.

1. Introduction

Perilla frutescens is an annual herbal plant belonging to the Lamiaceae family, and it is widely cultivated in Asian countries.[1] *P. frutescens* is an allotetraploid ($2n = 4x = 40$) species, and *P. citriodora* ($2n = 20$) is believed to be one of the diploid genome donors.[2] There are two chemotypes of perilla plants based on the content of anthocyanins: red and green perilla. Red perilla ("aka-shiso" in Japanese) is an anthocyanin-rich variety with dark red or purple leaves and stems, while green perilla ("ao-jiso" in Japanese) is an anthocyanin deficient variety with green leaves and stems.[3] Both green and red perilla leaves are often used as a material for cooking. Particularly, the leaves of red perilla are used as traditional Kampo medicine "soyou" to treat stomach problems,[1,2,4,5] and the seeds are also used to produce oil. Perilla seed oil is a rich source of α-linolenic acid, and its potential health benefits have been reported.[6,7]

Thus far, hundreds of bioactive compounds have been identified in *P. frutescens*,[1,8] among which perillaldehyde (monoterpenenoid) and rosmarinic acid (phenylpropanoid) are major phytochemicals.[9] Perillaldehyde has been shown to possess anti-inflammatory,[10] antidepressant,[11] antifungal, and antibacterial activities;[12,13] additionally, rosmarinic acid possesses antiviral, antibacterial, and anti-inflammatory activities.[14] Several enzymes for the biosynthesis of these compounds have been identified in *P. frutescens*. Perillaldehyde appears to be biosynthesized by the hydroxylation and subsequent oxidation of the C-7 position of limonene. Limonene synthase and a cytochrome P450 monooxygenase (P450) catalyzing the two-step oxidation of limonene at C-7 position have been cloned and characterized in *P. frutescens*.[15,16] Rosmarinic acid is proposed to be biosynthesized from 4-coumaroyl-CoA and 4-hydroxyphenyllactic acid.[17] Rosmarinic acid synthase, which is the first specific enzyme for rosmarinic acid biosynthesis, catalyzes the ester formation step of these two compounds. After 4-coumaroyl-4′-hydroxyphenyllactic acid formation, P450 enzymes belonging to the CYP98A family member are known to catalyze the final hydroxylation steps leading to rosmarinic acid production.[14,17] These enzymes have been cloned and characterized from several plant species, including *Coleus scutellarioides* (Lamiaceae); however, none has been identified in perilla plants.

Recently, genome editing tools, such as CRISPR-Cas9, have been used for the engineering of plant biosynthetic pathways.[18] For instance, deletion of the autoinhibitory domain of glutamate decarboxylase 3 (*GAD3*) using CRISPR-Cas9 technology promoted the accumulation of GABA (γ-aminobutyric acid) in tomato fruit, and this product is already commercially available.[19,20] Additionally, silencing of the potato sterol side chain reductase 2 (*SSR2*) by transcription activator-like effector nucleases (TALEN) suppressed the accumulation of toxic steroidal glycoalkaloids.[21] Therefore, genome sequencing and gene annotation could facilitate the identification of target genes to enhance desired traits, such as higher contents of valuable compounds and lower contents of unwanted compounds. Additionally, the genome of edited plants could be compared with that of the reference genome to identify the potential risk of off-target changes.[22,23] Long-read DNA sequencing technologies have emerged as powerful tools to obtain high-quality whole genome sequences.[24] Recently developed PacBio technology has facilitated the generation of high-fidelity (HiFi) reads from circular consensus sequencing (CCS), with long-read (> 10 kb) and high accuracy (> 99%).[24] In plant genome sequencing, highly contiguous near-chromosomal level sequences have been generated using HiFi

76 read-only.[25]

77 Here, we generated a highly contiguous genome assembly of red perilla (*P. frutescens*) domesticated in
78 Japan using PacBio HiFi reads. Functional annotation of identified genes was obtained using a systematic
79 functional annotation workflow optimized for plants. It is anticipated that the highly contiguous genome
80 assembly obtained in this study would promote the development of perilla varieties with desirable traits.
81

82 **2. Materials and methods**

83 **2.1. Sample preparation and genome sequencing**

84 DNA sample for genome sequencing was isolated from the young leaves of hydroponically grown *P. frutescens*
85 cv. Hoko-3 using a Genomic-tip kit (Qiagen, Hilden, Germany). Library preparation was performed using
86 SMRTbell Express Template Prep Kit 2.0 (PacBio, Menlo Park, CA, USA), and reads longer than 20 kb were
87 collected using BluePippin (Sage Science, Beverly, MA, USA). Thereafter, the libraries were sequenced using
88 Sequel IIe instrument (PacBio), and HiFi reads were selected from the circular consensus reads generated.
89

90 **2.2. Omni-C sequencing**

91 Dovetail Omni-C libraries were prepared using Omni-C kit (Dovetail Genomics, CA, USA), according to the
92 manufacturer's protocol. Sequencing was performed using DNBSEQ-G400 (MGI Tech, Shenzhen, China) in a
93 2 × 150 bp paired-end (PE) setting to obtain 356.34 million PE reads. The obtained reads were processed using
94 fastp v0.23.1 software[26] with default settings.
95

96 **2.3. *De novo* assembly of HiFi reads**

97 HiFi reads were assembled using Hifiasm v0.16.1[27,28] with the combination of processed Omni-C reads with --
98 hom-cov 55 --primary options (Hi-C integrated assembly).
99

100 **2.4. Quality assessment of genome assemblies**

101 Assembly statistics were obtained using QUAST v5.0.2[29]. Genome completeness was evaluated using BUSCO
102 v5.2.2 software[30] against embryophyta_odb10 (eukaryota, 2020-09-10) dataset (1,614 total BUSCO groups). *K*-
103 mer based assembly evaluation was performed using Merqury v1.3[31] and the Meryl db (k = 21) generated from
104 the HiFi reads.
105

106 **2.5. Omni-C scaffolding and construction of pseudochromosomes**

107 The processed Omni-C reads were mapped to the primary contigs generated by Hifiasm using BWA-MEM
108 v0.7.17,[32] followed by the removal of the 3′-side of the chimeric mapping and merging of the paired BAM files
109 using perl scripts from Arima Genomics mapping_pipeline
110 (https://github.com/ArimaGenomics/mapping_pipeline) and SAMtools v1.12.[33] The processed BAM file was
111 converted to BED format using BEDtools v2.30.0,[34] then scaffolding was performed using SALSA2 v2.3[35] with
112 -e DNASE -p yes options. To draw a Hi-C contact map, the output of SALSA2 was converted to .hic file using

113 convert.sh script equipped with SALSA2, then the generated .hic file was visualized using Juicebox v1.11.08[36].
114 A total of 25 scaffolds of 1 Mb or longer were extracted using SeqKit v2.0.0[37] and aligned with the 20
115 pseudochromosomes of the PF40 genome (GenBank assembly accession GCA_019511825.2[38]) using nucmer
116 sequence aligner with default settings and filtering of the delta alignment file with delta-filter command with -
117 q -r options in MUMmer4 v4.0.0rc1 package.[39] The alignment was drawn with a custom R script (original:
118 https://jmonlong.github.io/Hippocamplus/2017/09/19/mummerplots-with-ggplot2/). To create
119 pseudochromosomes based on the alignment with the PF40 genome, scaffold_19 and the reverse complement
120 sequences of scaffold_22 and scaffold_21 were joined in this order with gaps (500 Ns) to create a new scaffold
121 (scaffold_19). The longest 20 scaffolds (scaffold_1–20) of this assembly were renamed following the PF40
122 genome. Additionally, 10 of the 20 scaffolds (scaffold_2, 3, 6, 8, 13, 14, 15, 16, 17, and 18) were reverse
123 complemented to align with the PF40 genome in the same direction.
124
125 **2.6. Removal of organellar sequences**
126 The scaffolds were searched against chloroplast and mitochondrial genome sequences obtained from NCBI
127 RefSeq (all genomic sequences available at mitochondrion and plastid directories, as of November 8, 2021) by
128 blastn v2.12.0 with an E-value cutoff of 1e-5. Scaffolds with 90% or more coverage against one of the reference
129 organellar sequences were labeled as organellar scaffolds and removed from the primary assembly. All of the
130 scaffolds removed in this step were made from a single contig. We also performed the same organellar removal
131 procedure for the alternate haplotigs generated by Hifiasm.
132
133 **2.7. Transcriptome analysis**
134 Total RNA for PacBio isoform sequencing (Iso-Seq) was extracted from the mixed sample of leaves, stems, and
135 roots of the cultivar Hoko-3 using RNeasy Plant Mini kit (Qiagen, Hilden, Germany). Library preparation was
136 performed using NEBNext Single Cell/Low Input cDNA Synthesis & Amplification Module (New England
137 Biolabs, Ipswich, MA, USA) and SMRTbell Express Template Prep Kit 2.0 (PacBio). Thereafter, the reads
138 were sequenced using the Sequel IIe instrument (PacBio), and CCS reads were generated using SMRTLink
139 v10.0 (PacBio). The obtained BAM file was processed using IsoSeq v3.4.0 pipeline. Total RNA for RNA
140 sequencing (RNA-Seq) was extracted from leaves of the cultivar Hoko-3 using ISOSPIN Plant RNA kit (Nippon
141 Gene, Tokyo, Japan), and a sequencing library was prepared using NEBNext Poly(A) mRNA Magnetic
142 Isolation Module (New England Biolabs) and NEBNext Ultra Directional RNA Library Prep Kit for Illumina
143 (New England Biolabs). Sequencing was performed using NovaSeq 6000 (Illumina, San Diego, CA, USA) in a
144 2 × 150 bp paired-end (PE) setting. Reads from three biological replicates (154.20 million PE reads in total)
145 were combined and used for gene prediction and annotation.
146
147 **2.8. Gene prediction and annotation**
148 The processed Iso-Seq reads (high-quality isoforms) were mapped to the assembled genome using minimap2
149 v2.23,[40] then collapsed to obtain non-redundant isoforms using Cupcake ToFU scripts on cDNA_Cupcake

150 v28.0.0 (https://github.com/Magdoll/cDNA_Cupcake). The RNA-Seq reads were processed using fastp v0.23.2
151 with default settings, mapped to the assembled genome using HISAT2 v2.2.1,[41] and then transcript models were
152 constructed using StringTie v2.2.1.[42] Coding sequences from these two annotations were identified using
153 GenomeTools v1.6.2,[43] and gene features were obtained using a custom python script. The RNA-Seq reads were
154 mapped to the assembled genome to predict protein-coding genes using BRAKER2 v2.1.6.[44] For the input of
155 BRAKER2, the assembled genome was repeat masked using RepeatModeler v2.0.2 and RepeatMasker v4.1.2
156 in Dfam TE Tools Container v1.4 (https://github.com/Dfam-consortium/TETools). To merge the annotations
157 from Iso-Seq and RNA-Seq, non-overlapping gene features from RNA-Seq with those of Iso-Seq were obtained
158 using BEDtools v2.30.0 intersect (-s and -v options), then concatenated with the annotations from Iso-Seq after
159 removal of incomplete gene features using a custom python script. Similarly, non-overlapping gene features
160 from BRAKER2 against those of the combined Iso-Seq and RNA-Seq were merged to obtain the combined
161 gene annotations of Iso-Seq, RNA-Seq, and BRAKER2. The combined gene annotations were used for further
162 analysis including functional annotation.
163
164 **2.9. Functional annotation**
165 Functional annotation of the protein-coding genes on the primary assembly was performed using
166 Fanflow4Plants, designed for the functional annotation of plant species based on Fanflow4Insects.[45] In the
167 functional annotation of these protein coding sequences, these sequences were searched by GGSERACH
168 v36.3.8g in the FASTA package (https://fasta.bioch.virginia.edu/). Instead of *Caenorhabditis elegans* and
169 *Drosophila melanogaster* which were used as references in Fanflow4Insects, functionally well-curated protein
170 datasets of *Arabidopsis thaliana*, *Oryza sativa*, and *Solanum lycopersicum*, as well as UniProtKB/Swiss-Prot,
171 *Homo sapiens*, and *Mus musculus* were used as a reference (Supplementary Table S1). The sequences were also
172 searched by HMMSCAN in HMMER package v3.3.2 (http://hmmer.org/) against the hidden Markov model
173 (HMM) profile libraries of Pfam database v35.0.[46]
174
175 **3. Results**
176 **3.1. *De novo* assembly of red perilla cultivar Hoko-3**
177 We performed *de novo* assembly of the red perilla cultivar Hoko-3 (Fig. 1) from 72.4 Gb (57.5× coverage) of
178 PacBio HiFi reads using Hifiasm. Hi-C (Omni-C) integrated assembly of Hifiasm was performed by combining
179 the Omni-C reads and "--primary" option to generate primary and alternate contigs, as well as fully phased
180 haplotype 1 and 2 contigs. We specified the homozygous coverage in the parameter setting of Hifiasm (--hom-
181 cov 55) because the default setting could misidentify the coverage threshold for homozygous reads. The Hifiasm
182 outputs generated 317 primary contigs and 14,150 alternate contigs (Supplementary Table S2). *K*-mer
183 evaluation using Merqury showed that fully phased haplotype 1 and 2 were almost identical (Supplementary
184 Fig. S1); therefore, we did not distinguish the fully phased haplotypes for further analysis. Merqury analysis
185 indicated high base accuracy (QV = 60.1) and completeness (98.3%) of the primary contigs (Supplementary
186 Table S2).

187 Additionally, the Omni-C reads were mapped to the primary contigs, and then scaffolding was
188 performed using SALSA2 to construct pseudochromosomes. A total of 298 scaffolds were generated from the
189 319 primary contigs (two contigs were broken during the scaffolding), among which 25 were longer than 1 Mb
190 (Supplementary Table S3). The 25 scaffolds (> 1 Mb) were aligned against the previously assembled
191 chromosome-scale genome of green perilla cultivar PF40[38] using MUMmer4 (Supplementary Fig. S2). Among
192 the longest 20 scaffolds (scaffold_1–20), 19 (except for scaffold_19) covered each chromosome of the PF40
193 genome. Scaffold_19 partially covered chromosome 15 of the PF40 genome, and two other scaffolds
194 (scaffold_21 and 22) partially aligned with chromosome 15 of the PF40 genome (Supplementary Fig. S2).
195 Similarly, Hi-C contact map indicated that the three scaffolds (scaffold_19, 21, and 22) corresponded to the
196 same chromosome (Supplementary Fig. S3); therefore, the three scaffolds were combined based on their partial
197 alignment to chromosome 15 of the PF40 genome. We renamed and sorted the scaffolds based on the alignment
198 with the PF40 genome to construct 20 pseudochromosomes (Fig. 2). After removal of scaffolds predicted to be
199 derived from mitochondria or chloroplast genome, we obtained 71 scaffolds with N50 of 63.3 Mb
200 (Pfru_yukari_1.0; Table 1). The N50 value of the scaffolds was almost similar to that of the PF40 assembly;
201 however, the N50 value of the contigs was 41.5 Mb, which was ten times more than that of the PF40 assembly
202 (Table 1). Each of the 20 pseudochromosomes consisted of less than six contigs, of which seven
203 pseudochromosomes consisted of only one contig, indicating a highly contiguous genome assembly
204 (Supplementary Table S4). Additionally, 99.2 % of the assembly was assigned to 20 pseudochromosomes
205 (Supplementary Table S4). Completeness of the genome assembly evaluated with benchmarking universal
206 single-copy orthologs (BUSCO) (Manni *et al.*, 2021) showed that the assembly achieved almost complete
207 coverage of the BUSCO core gene sets (99.5% completeness) (Table 1). For the 14,150 alternate contigs
208 produced by Hifiasm, we removed sequences predicted to be derived from mitochondria or chloroplast genome,
209 and the obtained 12,627 contigs were deposited in DDBJ.
210
211 **3.2. Annotation of the Hoko-3 genome**
212 The length of repetitive sequences in the Hoko-3 genome was 866.7 Mb (68.84% of the genome) (Table 2).
213 Long terminal repeat (LTR) elements accounted for 37.07% of the genome, with Copia and Gypsy constituting
214 14.01 and 14.92%, respectively (Table 2). Gene annotation of the Hoko-3 genome was performed by merging
215 the gene models generated by Iso-Seq and RNA-Seq data, and gene prediction using BRAKER2 in this order.
216 A total of 86,258 gene models were predicted with the 98.7% BUSCO complete data (Table 3). Iso-Seq, RNA-
217 Seq, and BRAKER2 alone gave 66.7%, 97.0%, and 98.5% of BUSCO completeness, respectively
218 (Supplementary Table S5). Although the Iso-Seq alone gave fewer number of genes (19,452 genes) and lower
219 BUSCO completeness from the 33,869 transcripts (Supplementary Table S5), the combination of the Iso-Seq
220 and RNA-Seq gave higher BUSCO completeness (97.7%), and addition of the predicted model from BRAKER2
221 achieved 98.7% BUSCO completeness (Table 3), suggesting that genes and isoforms identified in Iso-Seq
222 contributed the higher completeness of the predicted gene models. The gene models were subjected to
223 Fanflow4Plants, designed for the functional annotation of plant species based on Fanflow4Insects. Among the

86,258 gene models, 76,825 gene models were predicted as protein-coding genes, among which 72,983 gene models were annotated to at least one of the reference sequences in GGSERACH or pfam domain by HMMSCAN (Table 4).

3.3. Identification of the genes related to specialized metabolites in Hoko-3

As a practical example of genome editing target selection, enzyme coding genes in the anthocyanin biosynthetic pathway were studied. The major anthocyanin in *P. frutescens* is malonylshisonin, which is a glycosylated form of cyanidin.[3] After the curation of the genes, the number of enzyme coding genes in the anthocyanin biosynthetic pathway in the genome were listed, including putative isoforms (Fig. 3, Supplementary Table S6). There were multiple copies of enzyme genes upstream of the pathway in the genome, but downstream enzyme genes were encoded in only a few locations in the genome. Based on this observation, it could be concluded that genes downstream of the pathway are most likely targets for genome editing to engineer the anthocyanin biosynthetic pathway in *P. frutescens*.

4. Discussion

Here, we generated a chromosome-level genome assembly of *P. frutescens* domesticated in Japan, using PacBio HiFi reads. Seven of the 20 pseudochromosomes were composed of only one contig, and the other pseudochromosomes were composed of not more than five contigs (Supplementary Table S4), indicating that the contigs generated from HiFi reads achieved a near-complete chromosome level. Recently, near-complete chromosome level assembly of *Macadamia jansenii* genome was generated from HiFi reads, with eight of the 14 pseudochromosomes represented by a single large contig,[25] which is comparable to our assembly. Although it is difficult to construct complete chromosomal-level genome assembly from HiFi read-only, it is now possible to obtain near-complete chromosome-level assembly simply by running a HiFi read assembler, including Hifiasm. Additionally, in the scaffolding process using Omni-C reads, chromosome 15 was separated into three scaffolds. This is possibly due to some structural differences preventing these scaffolds from joining into a single sequence.

The number of gene models annotated in this study by combining two evidence-based annotations (Iso-Seq and RNA-Seq) and the gene prediction method (BRAKER2) was 86,258 (Table 3), which is almost twice the previously assembled *P. frutescens* genome (43,527 genes)[38] and close to the number of genes reported in another Lamiaceae tetraploid species *Salvia splendens* (88,489 genes).[47] The gene models generated in the present study achieved extremely high BUSCO completeness (98.7%) (Table 3), indicating that the models could be valuable resources for gene functional analysis of *P. frutescens*. Furthermore, an annotation system named Fanflow4Plants was developed based on the Fanflow4Insects for the functional annotation of gene models.[45] Only well-curated protein datasets were used as references in this system to obtain reliable functional annotations, including protein sequences of three plant species (Arabidopsis, rice, and tomato) and two mammalian species (human and mouse), as well as UniProtKB/Swiss-Prot. Overall, 72,339 of 76,825 (94.2%) protein-coding genes were functionally annotated to at least one of the reference sequences (Table 4).

261 Since *P. frutescens* is a rich source of several metabolites,[1,8] metabolic engineering could be used to
262 enhance the biosynthesis and accumulation of valuable compounds in this species. Although genome editing of
263 *P. frutescens* has not yet been reported, recent advances have shown that genome editing could be done using
264 *Agrobacterium*-mediated transformation.[48] In the present study, potential targets of genome editing to
265 manipulate the anthocyanin biosynthetic pathway were identified (Fig. 3). As anthocyanin and rosmarinic acid
266 share the upstream biosynthetic pathway towards 4-coumaroyl-CoA, it could be possible to change the
267 metabolic flux into the biosynthesis of rosmarinic acid by knocking down the specific pathway for anthocyanin
268 biosynthesis. Similar approaches could be used to identify target genes to enhance the biosynthesis of
269 perillaldehyde or other beneficial compounds by examining the functional annotation of this genome assembly.
270 Additionally, further analysis showed that the *P. frutescens* cv. Hoko-3 possessed a highly homozygous genome
271 (Supplementary Fig. S1), which could be due to the fact that *P. frutescens* is a self-fertilizing crop.[49] This
272 homozygosity would be beneficial for the selection of unique targets for genome editing. Overall, our genome
273 assembly and annotation could serve as a unique resource for future genome editing studies of *P. frutescens*.
274

Acknowledgements

We thank Masaki Kurao (Hiroshima Prefectural Technology Research Institute) for technical assistance. This work was supported by Hiroshima Prefectural Government, the Center of Innovation for Bio-Digital Transformation (BioDX), an open innovation platform for industry-academia co-creation of JST (COI-NEXT, JPMJPF2010) and JSPS KAKENHI Grant 21K19118 to HB. Computations were partially performed on the NIG supercomputer at ROIS National Institute of Genetics.

Author contributions

Conceptualization: KO, HB, YN
Methodology: KT, YT, MS, TM
Software: KT, YT, MS, HB
Validation: KT, YT, MS
Formal analysis: KT, YT, MS, HB
Investigation: KT, YT, MS, HB, SM
Resources: KT, YT, MS, HB, SM, YK, TI
Data Curation: KT, YT, MS, HB
Writing - Original Draft: KT
Writing - Review & Editing: MS, YT, TM, SM, YK, TI, KO, YN, HB
Visualization: KT, YT, MS, HB
Supervision: YN, HB
Project administration: HB
Funding acquisition: KO, HB

Conflict of interest

The authors declare no conflict of interest.

Data availability statement

All sequencing data (assembled sequences and raw sequence reads) have been deposited in DDBJ under umbrella BioProject accession number PRJDB14288. The genome assembly from primary contigs has been deposited in DDBJ under the accession numbers BRKX01000001 to BRKX01000071. A set of haplotigs only sequences have been deposited in DDBJ under the accession numbers BRKY01000001 to BRKY01012627. The raw sequence reads have been deposited in DDBJ under the accession numbers DRR361636 (PacBio HiFi reads), DRR361637 (PacBio Iso-Seq reads), DRR361638 (Illumina RNA-Seq reads), and DRR415374 (Omni-C reads). Gene annotation and functional annotation of the protein coding genes are available at figshare (https://doi.org/10.6084/m9.figshare.20780995). Custom scripts used in this study are available at figshare (https://doi.org/10.6084/m9.figshare.20781466).

312

313 **Supplementary data**

314 Supplementary data are available at figshare (https://doi.org/10.6084/m9.figshare.20780419).

315

316 **Legends for supplementary data**

317 **Supplementary Table S1.** Source of protein-level functional annotation of Pfru_yukari_1.0.

318 **Supplementary Table S2.** Statistics of the contigs generated by Hifiasm.

319 **Supplementary Table S3.** AGP file (scaffolds_FINAL.agp) generated by SALSA2 describing the contig
320 assignment of each scaffold.

321 **Supplementary Table S4.** Length and the components of 20 pseudochromosomes.

322 **Supplementary Table S5.** Summary of the gene annotation of each of the three methods.

323 **Supplementary Table S6.** The GGSERACH results corresponds to the identified genes in Figure 3.

324 **Supplementary Figure S1.** Merqury assembly spectrum plots of haplotype 1 (hap1) and haplotype 2 (hap2).

325 **Supplementary Figure S2.** Dot-plot alignment between the draft scaffolds (indicated as "s") (longest 25
326 scaffolds; scaffold_1–25) and reference PF40 genome assembly. Blue dots represent +/+ strand alignments and
327 red dots represent +/- strand alignments.

328 **Supplementary Figure S3.** Hi-C contact map of the draft scaffolds (indicated as "s") generated by SALSA2.

329

330

331 **References**

332 1. Ahmed, H. M. 2019, Ethnomedicinal, phytochemical and pharmacological investigations of *Perilla*
333 *frutescens* (L.) Britt. *Molecules*, **24**, 102.
334 2. Nitta, M., Lee, J. K., Kang, C. W., et al. 2005, The distribution of *Perilla* species. *Genet. Resour.*
335 *Crop Evol.*, **52**, 797–804.
336 3. Saito, K., and Yamazaki, M. 2002, Biochemistry and molecular biology of the late-stage of
337 biosynthesis of anthocyanin: lessons from *Perilla frutescens* as a model plant. *New Phytol.*, **155**, 9–23.
338 4. Ueda, H., Yamazaki, C., and Yamazaki, M. 2002, Luteolin as an anti-inflammatory and anti-allergic
339 constituent of *Perilla frutescens*. *Biol. Pharm. Bull.*, **25**, 1197–202.
340 5. Deguchi, Y., and Ito, M. 2020, Rosmarinic acid in *Perilla frutescens* and perilla herb analyzed by
341 HPLC. *J. Nat. Med.*, **74**, 341–52.
342 6. Longvah, T., Deosthale, Y. G., and Uday Kumar, P. 2000, Nutritional and short term toxicological
343 evaluation of Perilla seed oil. *Food Chem.*, **70**, 13–6.
344 7. Hashimoto, M., Matsuzaki, K., Hossain, S., et al. 2021, Perilla seed oil enhances cognitive function
345 and mental health in healthy elderly Japanese individuals by enhancing the biological antioxidant potential.
346 *Foods*, **10**, 1130.
347 8. Hou, T., Netala, V. R., Zhang, H., Xing, Y., Li, H., and Zhang, Z. 2022, *Perilla frutescens*: A rich
348 source of pharmacological active compounds. *Molecules*, **27**, 3578.
349 9. Yoshida, H., Nishikawa, T., Hikosaka, S., and Goto, E. 2021, Effects of nocturnal UV-B irradiation
350 on growth, flowering, and phytochemical concentration in leaves of greenhouse-grown red perilla. *Plants*, **10**,
351 1252.
352 10. Uemura, T., Yashiro, T., Oda, R., et al. 2018, Intestinal anti-inflammatory activity of perillaldehyde.
353 *J. Agric. Food Chem.*, **66**, 3443–8.
354 11. Ji, W.-W., Wang, S.-Y., Ma, Z.-Q., et al. 2014, Effects of perillaldehyde on alternations in serum
355 cytokines and depressive-like behavior in mice after lipopolysaccharide administration. *Pharmacol. Biochem.*
356 *Behav.*, **116**, 1–8.
357 12. Sato, K., Krist, S., and Buchbauer, G. 2006, Antimicrobial effect of trans-cinnamaldehyde, (–)-
358 perillaldehyde, (–)-citronellal, citral, eugenol and carvacrol on airborne microbes using an airwasher. *Biol.*
359 *Pharm. Bull.*, **29**, 2292–4.
360 13. Tian, J., Wang, Y., Lu, Z., et al. 2016, Perillaldehyde, a promising antifungal agent used in food
361 preservation, triggers apoptosis through a metacaspase-dependent pathway in *Aspergillus flavus*. *J. Agric.*
362 *Food Chem.*, **64**, 7404–13.
363 14. Petersen, M., and Simmonds, M. S. J. 2003, Rosmarinic acid. *Phytochemistry*, **62**, 121–5.
364 15. Yuba, A., Yazaki, K., Tabata, M., Honda, G., and Croteau, R. 1996, cDNA cloning, characterization,
365 and functional expression of 4S-(–)-limonene synthase from *Perilla frutescens*. *Arch. Biochem. Biophys.*, **332**,
366 280–7.
367 16. Fujiwara, Y., and Ito, M. 2017, Molecular cloning and characterization of a *Perilla frutescens*

368 cytochrome P450 enzyme that catalyzes the later steps of perillaldehyde biosynthesis. *Phytochemistry*, **134**,
369 26–37.
370 17. Trócsányi, E., György, Z., and Zámboriné-Németh, É. 2020, New insights into rosmarinic acid
371 biosynthesis based on molecular studies. *Curr. Plant Biol.*, **23**, 100162.
372 18. Nishida, K., and Kondo, A. 2021, CRISPR-derived genome editing technologies for metabolic
373 engineering. *Metab. Eng.*, **63**, 141–7.
374 19. Nonaka, S., Arai, C., Takayama, M., Matsukura, C., and Ezura, H. 2017, Efficient increase of ɣ-
375 aminobutyric acid (GABA) content in tomato fruits by targeted mutagenesis. *Sci. Rep.*, **7**, 7057.
376 20. Ezura, H. 2022, Letter to the editor: The world's first CRISPR tomato launched to a Japanese market:
377 The social-economic impact of its implementation on crop genome editing. *Plant Cell Physiol.*, **63**, 731–3.
378 21. Sawai, S., Ohyama, K., Yasumoto, S., et al. 2014, Sterol side chain reductase 2 is a key enzyme in the
379 biosynthesis of cholesterol, the common precursor of toxic steroidal glycoalkaloids in potato. *Plant Cell*, **26**,
380 3763–74.
381 22. Graham, N., Patil, G. B., Bubeck, D. M., et al. 2020, Plant genome editing and the relevance of off-
382 target changes. *Plant Physiol.*, **183**, 1453–71.
383 23. Sturme, M. H. J., van der Berg, J. P., Bouwman, L. M. S., et al. 2022, Occurrence and nature of off-
384 target modifications by CRISPR-Cas genome editing in plants. *ACS Agric. Sci. Technol.*, **2**, 192–201.
385 24. Logsdon, G. A., Vollger, M. R., and Eichler, E. E. 2020, Long-read human genome sequencing and
386 its applications. *Nat. Rev. Genet.*, **21**, 597–614.
387 25. Sharma, P., Masouleh, A. K., Topp, B., Furtado, A., and Henry, R. J. 2022, *De novo* chromosome
388 level assembly of a plant genome from long read sequence data. *Plant J.*, **109**, 727–36.
389 26. Chen, S., Zhou, Y., Chen, Y., and Gu, J. 2018, fastp: an ultra-fast all-in-one FASTQ preprocessor.
390 *Bioinformatics*, **34**, i884–90.
391 27. Cheng, H., Concepcion, G. T., Feng, X., Zhang, H., and Li, H. 2021, Haplotype-resolved *de novo*
392 assembly using phased assembly graphs with hifiasm. *Nat. Methods*, **18**, 170–5.
393 28. Cheng, H., Jarvis, E. D., Fedrigo, O., et al. 2022, Haplotype-resolved assembly of diploid genomes
394 without parental data. *Nat. Biotechnol.*, 1332–5.
395 29. Mikheenko, A., Prjibelski, A., Saveliev, V., Antipov, D., and Gurevich, A. 2018, Versatile genome
396 assembly evaluation with QUAST-LG. *Bioinformatics*, **34**, i142–50.
397 30. Manni, M., Berkeley, M. R., Seppey, M., Simão, F. A., and Zdobnov, E. M. 2021, BUSCO Update:
398 Novel and streamlined workflows along with broader and deeper phylogenetic coverage for scoring of
399 eukaryotic, prokaryotic, and viral genomes. *Mol. Biol. Evol.*, **38**, 4647–54.
400 31. Rhie, A., Walenz, B. P., Koren, S., and Phillippy, A. M. 2020, Merqury: reference-free quality,
401 completeness, and phasing assessment for genome assemblies. *Genome Biol.*, **21**, 245.
402 32. Li, H. 2013, Aligning sequence reads, clone sequences and assembly contigs with BWA-MEM. *arXiv*,
403 1303.3997.
404 33. Li, H., Handsaker, B., Wysoker, A., et al. 2009, The sequence alignment/map format and SAMtools.

405 *Bioinformatics*, **25**, 2078–9.
406 34. Quinlan, A. R., and Hall, I. M. 2010, BEDTools: a flexible suite of utilities for comparing genomic
407 features. *Bioinformatics*, **26**, 841–2.
408 35. Ghurye, J., Rhie, A., Walenz, B. P., et al. 2019, Integrating Hi-C links with assembly graphs for
409 chromosome-scale assembly. *PLoS Comput. Biol.*, **15**, e1007273.
410 36. Durand, N. C., Robinson, J. T., Shamim, M. S., et al. 2016, Juicebox provides a visualization system
411 for Hi-C contact maps with unlimited zoom. *Cell Syst.*, **3**, 99–101.
412 37. Shen, W., Le, S., Li, Y., and Hu, F. 2016, SeqKit: A cross-platform and ultrafast toolkit for FASTA/Q
413 file manipulation. *PLoS One*, **11**, e0163962.
414 38. Zhang, Y., Shen, Q., Leng, L., et al. 2021, Incipient diploidization of the medicinal plant *Perilla*
415 within 10,000 years. *Nat. Commun.*, **12**, 5508.
416 39. Marçais, G., Delcher, A. L., Phillippy, A. M., Coston, R., Salzberg, S. L., and Zimin, A. 2018,
417 MUMmer4: A fast and versatile genome alignment system. *PLoS Comput. Biol.*, **14**, e1005944.
418 40. Li, H. 2018, Minimap2: pairwise alignment for nucleotide sequences. *Bioinformatics*, **34**, 3094–100.
419 41. Kim, D., Paggi, J. M., Park, C., Bennett, C., and Salzberg, S. L. 2019, Graph-based genome alignment
420 and genotyping with HISAT2 and HISAT-genotype. *Nat. Biotechnol.*, **37**, 907–15.
421 42. Pertea, M., Pertea, G. M., Antonescu, C. M., Chang, T.-C., Mendell, J. T., and Salzberg, S. L. 2015,
422 StringTie enables improved reconstruction of a transcriptome from RNA-seq reads. *Nat. Biotechnol.*, **33**, 290–
423 5.
424 43. Gremme, G., Steinbiss, S., and Kurtz, S. 2013, GenomeTools: A comprehensive software library for
425 efficient processing of structured genome annotations. *IEEE/ACM Trans. Comput. Biol. Bioinform.*, **10**, 645–
426 56.
427 44. Brůna, T., Hoff, K. J., Lomsadze, A., Stanke, M., and Borodovsky, M. 2021, BRAKER2: automatic
428 eukaryotic genome annotation with GeneMark-EP+ and AUGUSTUS supported by a protein database. *NAR*
429 *Genomics Bioinforma.*, **3**, lqaa108.
430 45. Bono, H., Sakamoto, T., Kasukawa, T., and Tabunoki, H. 2022, Systematic functional annotation
431 workflow for insects. *Insects*, **13**, 586.
432 46. Mistry, J., Chuguransky, S., Williams, L., et al. 2021, Pfam: The protein families database in 2021.
433 *Nucleic Acids Res.*, **49**, D412–9.
434 47. Jia, K.-H., Liu, H., Zhang, R.-G., et al. 2021, Chromosome-scale assembly and evolution of the
435 tetraploid *Salvia splendens* (Lamiaceae) genome. *Hortic. Res.*, **8**, 177.
436 48. Kim, K.-H., Lee, Y.-H., Kim, D., et al. 2004, *Agrobacterium*-mediated genetic transformation of
437 *Perilla frutescens*. *Plant Cell Rep.*, **23**, 386–90.
438 49. Sa, K. J., Kim, J. A., and Lee, J. K. 2012, Comparison of seed characteristics between the cultivated
439 and the weedy types of *Perilla* species. *Hortic. Environ. Biotechnol.*, **53**, 310–5.
440
441

442 **Tables**

443 **Table 1.** Statistics of the genome assembly of red perilla cultivar Hoko-3 (Pfru_yukari_1.0) in comparison with
444 the previous assembly of the PF40 genome (ICMM_Pfru_2.0)

	Pfru_yukari_1.0	ICMM_Pfru_2.0
Total sequence length	1,258,994,547	1,234,370,464
No. of pseudochromosomes	20	20
No. of scaffolds	71	1,465
Scaffold N50	63,334,402	62,644,896
Scaffold L50	9	10
No. of contigs	94	2,228
Contig N50	41,459,669	2,738,655
Contig L50	11	137
Complete BUSCO[a] (%)	99.5	99.3
Complete and single-copy (%)	4.1	6.3
Complete and duplicated (%)	95.4	93.0

445 [a]embryophyta_odb10 (eukaryota, 2020-09-10) dataset (1,614 total BUSCO groups)

446

447 **Table 2.** Summary of repetitive elements in Pfru_yukari_1.0

	Length occupied (bp)	% of whole genome
Retroelements	474,789,418	37.71
LINEs	8,042,571	0.64
LTR elements	466,746,847	37.07
Copia	176,347,151	14.01
Gypsy	187,848,187	14.92
Others	102,551,509	8.15
DNA transposons	50,983,076	4.04
RC/Helitron	7,435,521	0.59
Unclassified	313,615,583	24.91
Total interspersed repeats	846,823,598	67.26
Small RNA	2,844,362	0.23
Low complexity	2,121,838	0.17
Simple repeats	14,903,442	1.18
Total	866,693,240	68.84

448

449 **Table 3.** Summary of the annotated genes

	Iso-Seq	Iso-Seq RNA-Seq	Iso-Seq RNA-Seq BRAKER2
No. of genes	19,452	53,541	86,258
No. of transcripts	33,869	88,890	121,996
Complete BUSCO[a]	66.7%	97.7%	98.7%
Complete and single-copy	26.5%	5.9%	5.3%
Complete and duplicated	40.2%	91.8%	93.4%

450 [a]embryophyta_odb10 (eukaryota, 2020-09-10) dataset (1,614 total BUSCO groups)

451

452

453 **Table 4.** Protein-level annotation of Pfru_yukari_1.0

Annotation Category	Annotation Level	Gene count
Protein homolog from tophit	Arabidopsis	54,262
	Rice	55,694
	Tomato	59,044
	Human	38,255
	Mouse	36,099
	UniProtKB/Swiss-Prot	52,566
	At least one of the above	72,339
No protein homolog	Protein domain	644
Total genes with protein-level annotation		72,983
Hypothetical protein		3,842
Total		76,825

454

455

456 **Figure legends**

457 **Figure 1.** An image of the *Perilla frutescens* cv. Hoko-3 used for genome sequencing

458 **Figure 2.** Dot-plot alignment between this genome assembly and reference PF40 genome assembly. Blue dots
459 represent +/+ strand alignments and red dots represent +/- strand alignments. The large (> 3 Mb) structural
460 differences detected in this alignment are eight inversions (two in chr02 and 08, and one in chr06, 09, 10, and
461 15), three gaps in PF40 genome (chr05, 08, and 16), and one rearrangement in chr04.

462 **Figure 3.** The number of enzyme coding genes in the representative anthocyanin biosynthetic pathway of *P.*
463 *frutescens*. PAL, phenylalanine ammonia-lyase; C4H, trans-cinnamate 4-monooxygenase; 4CL, 4-
464 coumarate:CoA ligase; CHS, chalcone synthase; CHI, chalcone-flavanone isomerase; F3H, flavanone 3-
465 hydroxylase; F3′H, flavonoid 3′-hydroxylase; DFR, dihydroflavonol 4-reductase; LDOX, leucoanthocyanidin
466 dioxygenase.

467

468

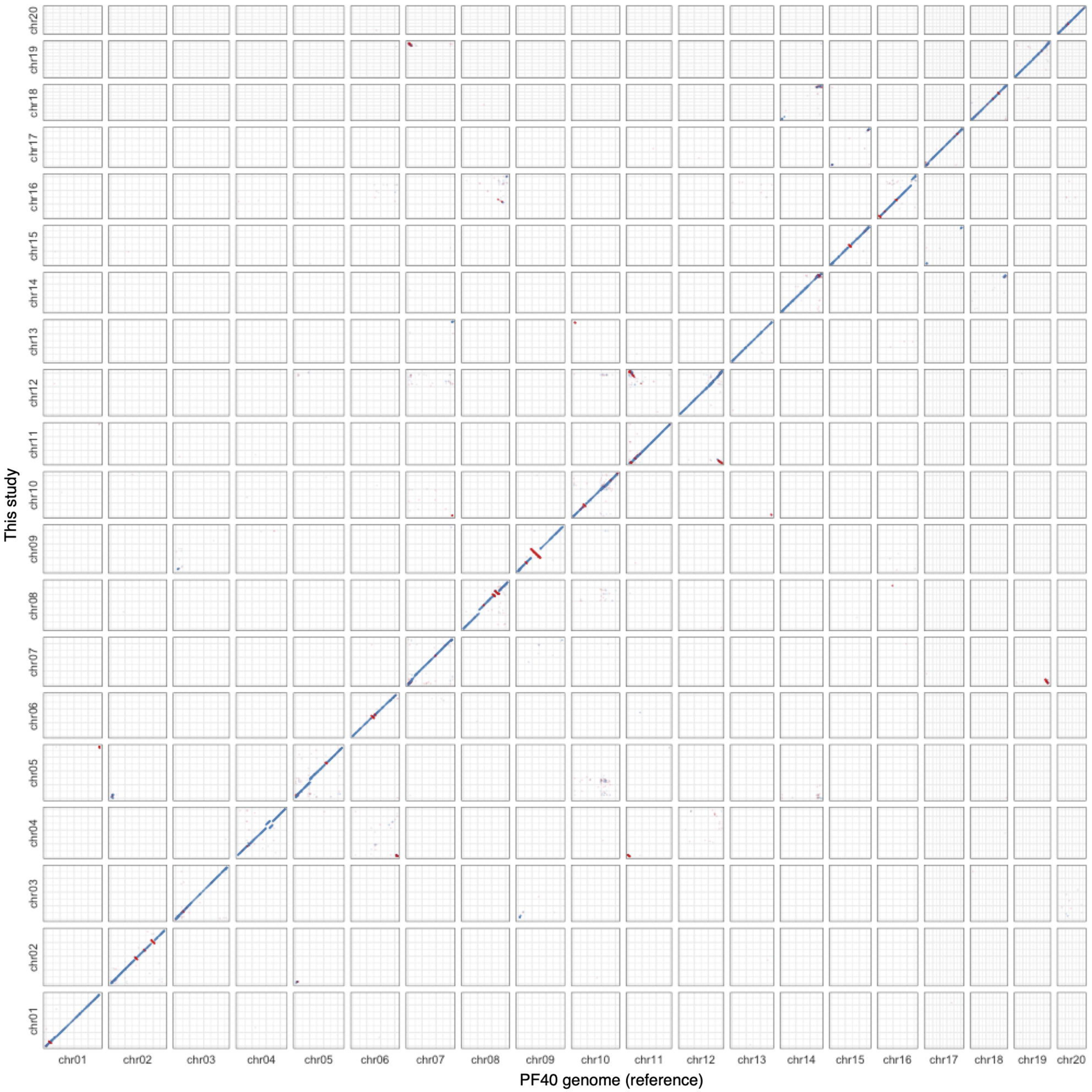
This study
chr01
chr02
chr03
chr04
chr05
chr06
chr07
chr08
chr09
chr10
chr11
chr12
chr13
chr14
chr15
chr16
chr17
chr18
chr19
chr20
PF40 genome (reference)

The number of enzyme coding genes in anthocyanin synthetic pathway of *P. frutescens*

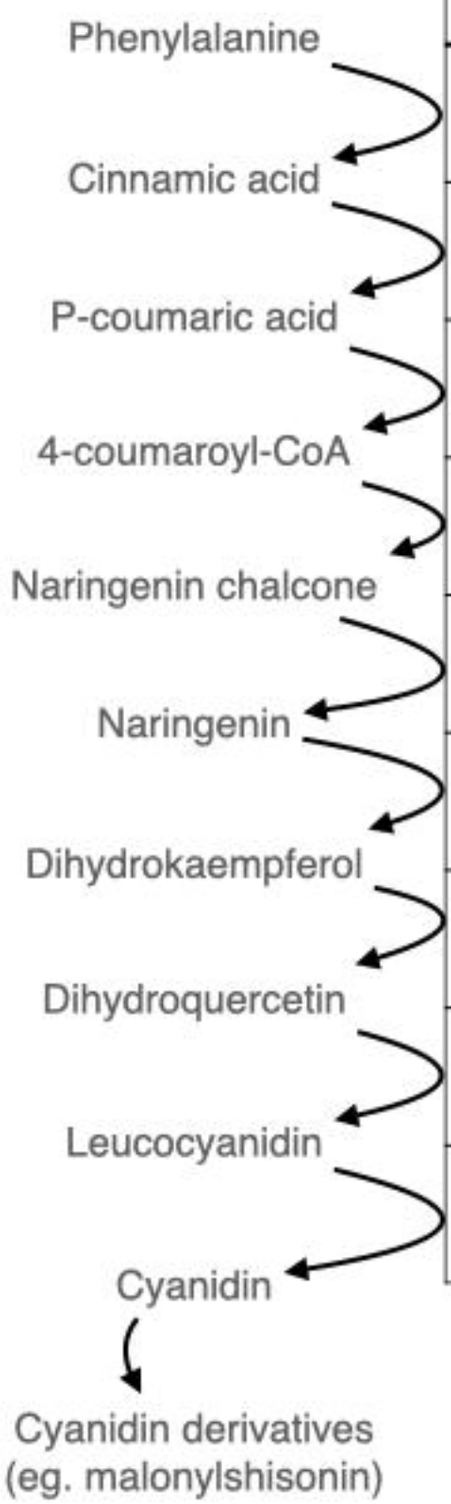

Enzyme	locus	isoform	RefUniProtKB
PAL1	6	17	PAL1_ARATH
C4H	8	12	TCMO_ARATH
4CL	7	17	4CL1_ARATH
CHS	17	23	CHSY_ARATH
CHI	2	2	CFI1_ARATH
F3H	2	2	FL3H_ARATH
F3'H	4	8	F3PH_ARATH
DFR	1	4	DFRA_ARATH
LDOX	2	3	LDOX_ARATH